Front. Chem. China 2010, 5(3): 288–298
DOI 10.1007/s11458-009-0210-9

FEATURE ARTICLE

Dissipative particle dynamic simulation study of lipid membrane

Shaogui WU[1,2], Teng LU[1] and Hongxia GUO (✉)[1]

1 Beijing National Laboratory for Molecular Sciences, Joint Laboratory of Polymer Sciences and Materials, State Key Laboratory of Polymer Physics and Chemistry, Institute of Chemistry, Chinese Academy of Sciences, Beijing 100190, China
2 College of Chemistry and Materials Sciences, Sichuan Normal University, Chengdu 610068, China

The lipid membrane plays crucial roles in countless biologic processes, ranging from cell motility, endo- and exocytosis, and cell division to protein aggregation and trafficking. To gain a molecular insight in these biologic processes, the recently developed mesoscale simulation technique, dissipative particle dynamics (DPD) simulation, has become an invaluable tool. By providing a brief survey of existing atomistic and popular coarse-grained models used today in studying the dynamics (including vesicle formation and (protein-mediated) vesicle fusion) and phase behavior of lipid bilayers, this review illustrates how mesoscopic DPD models can be used to obtain a better understanding of these biologic processes currently inaccessible to atomistic and most coarse-grained models.

Keywords dissipative particle dynamics, lipid membrane, vesicle fusion, 2D phase transformation

1 Introduction

It's well known that the cells are the essential structural and functional units of living organism [1]. To keep normal living activity, the composition of cells must be stable and the inside material should be maintained, therefore there should be some kinds of barrier between cells and the environment. These barriers are biologic membranes which play an important role in organism and are constituted by phospholipids, proteins and cholesterols. Today, biologic membranes are receiving ever-increasing attention from both theoretical and practical points of view. Phosphlipid is a class of natural amphiphiles, which contains a hydrophilic head group and one or two hydrophobic tails (hydrocarbon chains). Similar to surfactants or special types of block co-polymers, phosphlipid can self-assemble into a variety of interesting configurations in aqueous solution, such as spherical or rod-like micelles, bilayer membranes, vesicles, and even more complex structures [2–9]. Among these structures, vesicle is an enclosed bilayer structure with solvent molecules encapsulated inside. Because of their encapsulating ability, vesicle is useful in many applications, from drug delivery [10] and biosensor [11] to micro-reactor [12] and so on. More importantly, because vesicles are closely analog to biologic cells, they are studied widely as the model systems for biologic membranes [13]. Thus, an important first step to understand vesicle is to have a molecular-level understanding of vesicle formation, vesicle fusion and its fission. Also, among the major issue concerning the functions of the biologic membranes, it is important to examine 2D phase transformation in bilayer membrane. Now considerable efforts have been devoted by experimental and theoretical studies to deepen our understanding these relevant biologic phenomena [13–32].

The motion of lipid membranes spans a broad range of temporal and spatial scales, from femtosecond dynamics and atomistic detail to real-time macroscopic behavior extending to seconds [33]. Between these domains there is a gap at the mesoscale level spanning spatial scales of hundreds of nanometres to microns and temporal scales of hundreds of nanoseconds to milliseconds, which are relevant for collective

Received December 4, 2009; accepted January 12, 2010
E-mail: hxguo@iccas.ac.cn

motions [34]. In a biologic context, many events essential for biologic properties occur in the mesoscopic scale, i.e., domain formation, phase transformation, membrane fusion and fission, as well as membrane-protein interactions. However, it is not easy to investigate these important phenomena directly by conventional experimental methods [16]. On the other hand, it is quite arduous to obtain molecular insight from analytical theoretical approach [35–38]. With the aid of the increase in computational power, molecular simulations have become potential method to address the limitations of either analytical or experimental approaches [13,15,17–26]. Although the straightforward molecular dynamic (MD) simulations permit an atomic resolution, the computationally demanding leads to a huge difficulty in addressing many cooperative effects of biologic interest [21,22]. Therefore the study of these important collective mesoscopic motions in lipid membranes is eventually more amenable to coarse-grained (CG) molecular models using mesoscale computer-simulation techniques. Although some atomistic details are sacrificed by the CG procedure, the CG models incorporate most salient features (i.e. the tendency to unmixing and the connectivity) of lipids, and are capable of reproducing many essential physical characteristics in the targeted area of interest. This reduction in the number of degrees of freedom yields a tremendous computational speedup. More recently, a mesoscopic simulation technique-disspative particle dynamic (DPD) simulation that can treat much larger system sizes and much longer time scales than full atomistic MD simulations have been applied to the study of vesicle formation, 2D-phase transition and vesicle fusion and fission [13,39–48]. In such computer simulations, the molecules are allowed to move based only on the essential molecular properties and on the intermolecular interactions. In addition to this, the soft interaction potential leads to a further effective speed-up in simulation time. As such, the use of soft potentials and a reduced number of interaction sites make DPD simulation a valuable complement to both experimental and analytical approaches, and hence play an important role in unraveling the various dynamics, e.g., spontaneous vesicle formation, phase transformation, and fusion and fission of the vesicles at molecular level. In this paper, we describe the current progress on molecular simulations, especially DPD simulations, of vesicle formation and (protein-mediated) fusion, and 2D phase transformation in lipid membrane. We believe that this review may be helpful to provide a deep understanding of the general principles in dynamics and phase behavior of lipid membrane. The application of molecular simulation techniques to biologic membranes has also been the subject of several reviews [49–51], and a comparative reading of these will provide the interested readers with a more complete perspective on this field.

2 Vesicle formation

In general the discussion of vesicle formation and its further shape change is based on the assumption that the membrane is already formed [52–57], thus not allowing the molecular description of the aggregation mechanisms of amphiphiles forming vesicles. Until now this important feature is realized by the use of molecular simulations [13,15,17,19]. It has been proved that a bilayer structure is an important immediate for the spontaneous vesicle formation, but why a bilayer curls to form a vesicle is still a much-debated issue [13,17,19]. Bernardes studied the spontaneous vesicle formation using lattice Monte Carlo simulation [17]. He found that the total potential energy after the vesicle formation was higher than that in the initial state. Thus, he concluded that the bilayer-vesicle transition was driven by entropy. However, more information can be obtained from a detailed study of these energy curves. In the initial configuration, particles were orderly setup, hence at a rather low energy state. Subsequently, the unnatural starting conformation was relaxed during the thermo equilibration, which resulted in the promotion of the system energy. In the later bilayer-vesicle transition, energy curve displayed a small reduction (as shown in Figure 4 in reference [17]). Thus, it is insufficient to conclude that bilayer-vesicle transition was driven by entropy based on just comparing the energy of an “artificial initial state” with that of the final state. Later, Markvoort et al. studied the same issue and came into the same conclusion that the bilayer-vesicle transition is entropy driven [19]. Unfortunately, similar to what Bernardes mesaured, the increasing of energy only occurred in the earlier molecular relaxation stage rather than in the later bilayer-vesicle transition stage. Recently, Yamamoto investigated the spontaneous vesicle formation of amphiphilic molecules in aqueous solution using DPD simulation [13]. By monitoring the energy evolution, he deduced that reduction of hydrophobic energy might be the primary driving force for the bilayer-vesicle transition.

To further clear the driving force for vesicle formation, we performed a series of DPD simulations [58]. The coarse-grained model was constructed from the molecular architecture of DMPC lipid, denoted here as $h_3(t_5)_2$, wherein the head moiety is consisted of three hydrophilic beads (h, red) and two tails are consisted of five hydrophobic beads (t, green) each. Two initial configurations were adopted: a randomly dispersed solution and a tensionless bilayer. The pathway of the spontaneous vesicle formation from a randomly dispersed solution is shown in Figure 1. At the early stage, lipid molecules quickly aggregate into many small micelles. These small micelles then merge to form larger ones until a large oblate micelle (or bilayer) is formed. Subsequently, the bilayer curls to form a vesicle, with some water encapsulated inside

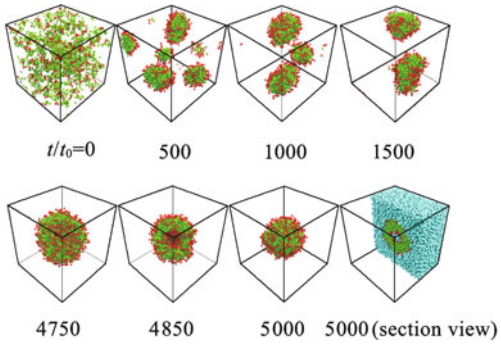

Figure 1 Spontaneous vesicle formation from a randomly dispersed solution [58].

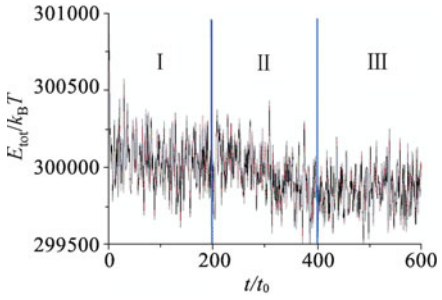

Figure 3 Time dependence of total energy E_{tot}. I: Bilayer thermal fluctuation stage. II: Bilayer curling and closing stage. III: Vesicle steady stage [58].

meanwhile. In a group of parallel simulations, it was found that once a large enough bilayer was formed, it would quickly curl to form a vesicle, confirming that bilayer is an important immediate for the spontaneous vesicle formation. To facilitate the study of molecular structures and pressure tensor changes during the bilayer-vesicle transition, we started our simulation from a circular tensionless bilayer directly, which was parallel to the *x*-*y* plane of the simulation box. Figure 2 displays the evolution pathway. The existence of the hydrophobic edge in the initial bilayer drives these "uncovered" tail particles quickly shielded by head particles in order to avoid the direct contact with water. In the subsequent time, the bilayer adjusts its conformation under the thermal fluctuation, but still keeps nearly circular shape. Then subtle bending occurs, which develops quickly, leading to the formation of a bowl-like quasi-vesicle. At the same time the mass center of bilayer moves out of the aggregate. At last, the pore in the quasi-vesicle is closed and water is encapsulated to generate a complete vesicle. By analyzing explicit interaction energy changes, we find that the total potential energy decreases during the bilayer-vesicle transition. As shown in Figure 3, during the period of $t = (200–400)t_0$, E_{tot} reduces significantly, correspondingly to the period of the bilayer-vesicle transition. To further probe the relation between energy changes and morphology evolution, the inter-particle energies have been measured. In present system, there are three types of particles: water (w), tail (t) and head (h), corresponding to six types of interaction energies: E_{ww}, E_{wt}, E_{wh}, E_{tt}, E_{th}, and E_{hh}. Among them, E_{wt} contributes most to the decreasing of E_{tot} and keeps pace with the change of E_{tot} during the bilayer-vesicle transition as shown in Figure 4. The decrease of E_{wt} is resulted from the reduction of number of w-t interaction pair n_{wt}, indicating that the water-tail interaction is weakened during the vesicle formation. Therefore the bilayer-vesicle transition is caused by the minimization of hydrophobic interaction between water-tail. On the other hand, n_{wh} decreases while n_{ww} and n_{hh} increase, suggesting that water molecules have been redistributed during the transition: the number of water in the proximity of the bilayer decreases but it increases in the bulk. The phenomenological theory assumes that, despite the bending energy increase upon the bilayer curling, the decreasing of edge size causes the reduction of edge energy, and finally leads to the reduction of the free energy. From the above analysis, we see that the reduction of free energy can be mainly attributed to the reduction of the hydrophobic energy. It is well known that thermodynamic observable like pressure is an important ingredient to monitor the dynamics, especially for a heterogeneous phase system. The change of pressure is indeed in one-to-one correspondence with that of E_{tot}. Compared with the initial state, pressure has descended to a certain extent. It implies that the vesicle is at a lower free energy state compared with a bilayer. The lower free energy is mainly due to the minimization of the hydrophobic energy between water and tail particles rather than the entropy growth caused by the redistribution of water molecules. The self-assembled bilayers exhibit stable fluid behavior. The derived structure properties such as lipid area (61Å^2) and bilayer thickness, as well as the measured area compression moduli $K_n = 428 \times 10^{-3}\,\mathrm{J\cdot m^{-2}}$

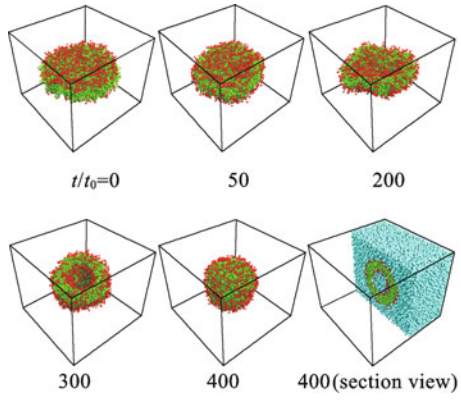

Figure 2 Pathway of spontaneous vesicle formation from a tensionless bilayer [58].

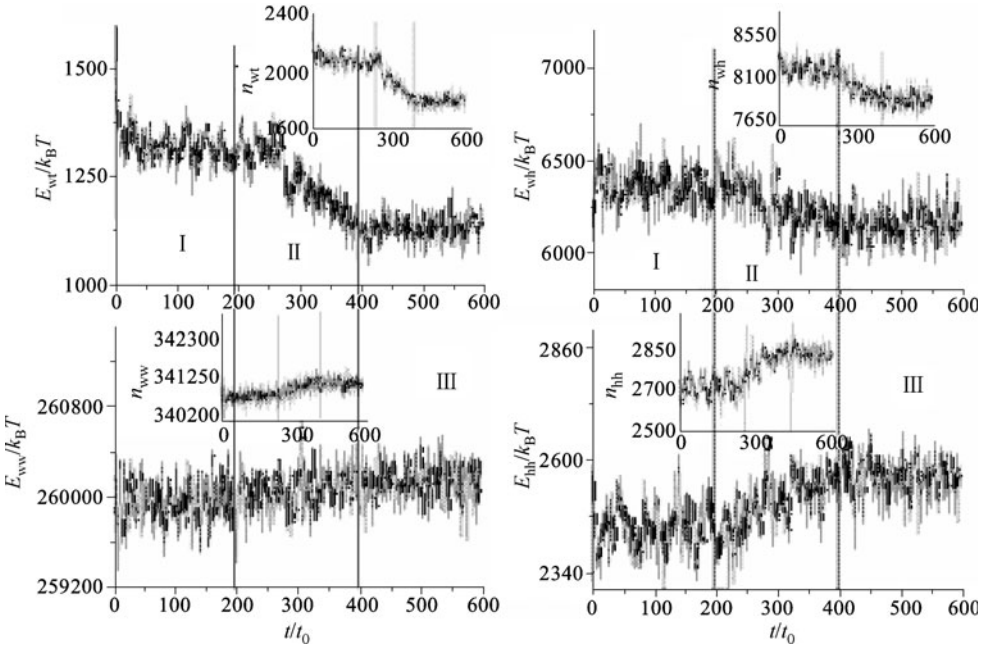

Figure 4 Time dependence of E_{wt}, E_{wh}, E_{ww}, E_{hh} and the corresponding particle interaction pair numbers [58].

and bending rigidity $\kappa = 22.35k_BT$ are well comparable to the lipid biologic membranes [59].

3 (Protein-mediated) vesicle fusion

Vesicle fusion is an important process in many biologic events, such as virus infection, membrane traffic, and sperm-egg binding and so on [60]. Due to membrane fusion occurring on a length scale of tens of nanometers and a time scale of submilliseconds [21], it is not easy to investigate the intermediate structures directly using conventional experimental approaches. Nowadays, computer simulations have been used in membrane fusion study, because they can track collective behavior at the molecular level [21,25,31,61–63]. Marrink et al. first investigated the mechanism of vesicle fusion using molecular dynamics simulation method based on coarse-grained lipid models [25]. Once the effective contact was established between two approaching vesicles, two fusion pathways were observed. The Pathway I is illustrated as following: First, the contacting region expands radically, giving rise to a so-called stalk intermediate. Then the center region of stalk is ruptured, which results in the merging of inner monolayers. This intermediate is termed as hemifusion diaphragm (HD) phase, which is stable before a small fusion pore appears. Eventually, the enlargement of the fusion pore and the degradation of HD complete the full fusion. This vesicle fusion pathway is in general agreement with the stalk-pore hypothesis [64]. In an alternative fusion pathway, some transient pores directly originate from the radically expanding stalk. Different from the fusion pore, these pores are small tunnels connecting the outer and inner monolayers. Consequently, lipids originally located in outer leaflets can flip-flop into the inner leaflet, leading to the mixing of monolayer content. This pathway is named "modified stalk-pore" mechanism.

Although the stalk model is well received, many different hypotheses on the molecular mechanisms of vesicle fusion exist as well [61,62,64,65]. Because these mechanisms cannot be readily asserted experimentally, Smeijers and coworkers addressed this problem using a coarse-grained molecular dynamics simulation [66]. They demonstrated that the stalk is initiated by lipid tails that extend spontaneously and evolve into a hydrophobic bridge. The stalk is composed of the contacting monolayers only, and never disintegrates once established. In all simulations, the fusion process is analogous, but the stalk evolution may differ. Typically, the stalk expands radically to enlarge the contact region. However, sometimes the stalk expands anisotropically into an elongated stalk, which grows and folds to form a stalk ring. However, what kind of stalk expansion is more favorable, the radial one leading to an HD or the anisotropic one resulting in an elongated connection? To answer this question, we studied the vesicle fusion with the dissipative particle dynamics simulation method. It is found that the whole fusion process in small vesicles is in well agreement with the radial stalk expansion route. Vesicle fusion is a process of energy minimization, which is mainly caused by the reduction of

water-amphiphile interaction energy. The decreasing of pressure during vesicle fusion confirms that the fused vesicle is at a lower free energy state. Typically, small vesicles fuse faster than large vesicles. For the large vesicles, even if the effective contacts are established, the fusion events seem to be trapped at the HD stage. Figure 5 gives a typical snapshot of HD stage. A fusion pore has not appeared within the observed time. Perhaps more time are needed to accomplish the "hemifusion-pore" transition. The difference may originate from the small curvature of large vesicles. When the curvature decreases, the contact zone becomes too large to direct an elongated stalk into a tight ring, and the vesicles trap in a hemifused state. The fusion events with large ones are therefore hard to proceed forward. Even the subsequent "hemifusion-pore" transition which is initiated by trigger events have a small chance of happening for large vesicles. Recently, Liang's group explored the fusion and fission pathways of vesicles composed by complex architecture amphiphile A-B-A and A-B-C and found two pathways for both fusion and fission processes [40,41].

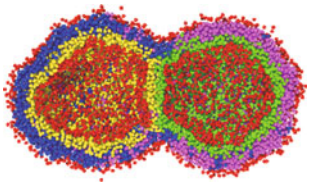

Figure 5 Section view for vesicle fusion trapped at the HD stage. (For clarity, water beads are omitted.) [39].

Research on fusion has been intense in recent years, but we are still far from a coherent molecular picture. For two vesicles to fuse, they must get close to establish an initial contact, which necessitates considerable energy to remove the water and dehydrate the polar head groups of lipids [27]. This is why membranes do not fuse spontaneously under normal circumstances, which requires special proteins and is subject to selective control [28]. These proteins mediate the initial recognition of the membranes destined for fusion, pull them together, destabilize the lipid/water interface, and trigger mixing of the lipids [29]. Several phenomenon models for protein-mediated membrane fusion have been proposed, such as Proteinaceous fusion pore model, Fence model, Scaffold model and Local perturbation model [30]. To get a full molecular understanding of the roles of fusion protein (i.e., SNARE, soluble *N*-ethylmaleimide-sensitive protein attachment protein receptor) in intracellular fusion reactions, we employed dissipative particle dynamics (DPD) simulation to study the complicated protein-mediated vesicle fusion involving extensive and cooperative molecular rearrangement. Model proteins (here termed as *t*- and V-proteins localizing in apposing vesicles) are designed according to the function of fusion proteins "SNAREs," in which the formation of a SNARE complex establishes membrane proximity, leading to complete fusion [67]. Following the model formulation of Venturoli et al. [68], the model protein is built from a bundle of seven amphiphile chains. Inclusion of a cap bead at the tip is for better coupling of *t*- and V-proteins. Furthermore, model proteins featured by multiblocks and self-defined interactions are imposed on the corresponding block pairs between *t*- and V-proteins. The interactions introduced here are just simply mimicking the specific interactions (i.e., helical hydrogen bonds, electrostatic interaction between charged residues) between multiple distinct binding sites of fusion protein pairs to form protein complexes.

The protein-mediated fusion is illustrated in Figure 6. The assembly of *t*- and V- protein pairs in the separate vesicles begins at the contacted caps down toward the membrane anchors, and forms into a parallel bundle like a zipper, which acts as the trans-SNARE complex to bridge apposed vesicles and supply the free energy needed for removal of water. More than one protein-complex is formed so as to generate large enough dragging force. By gradually binding the specific blocks one another in the pairing proteins, complexes tightly drag the apposing vesicles proximally. The subsequent route is completely consistent with the stalk-pore hypothesis [64]: at first, the initial contact between proximal monolayers grows outwards to form a so-called stalk intermediate. Second, the

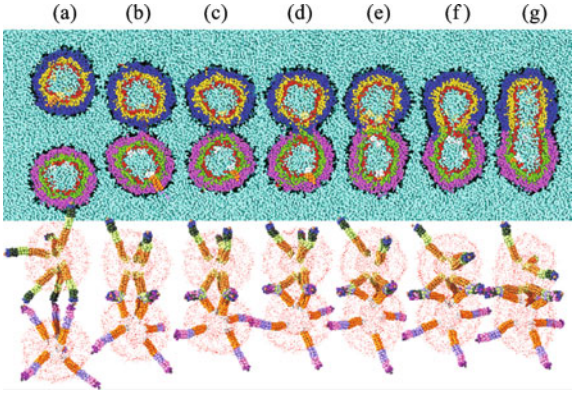

Figure 6 Pathway I of protein-mediated vesicle fusion (Scaffold model). (a) $0t_0$, starting state; (b) $355t_0$, outer leaflets contact; (c) $385t_0$, stalk; (d) $400t_0$, inner leaflets contact; (e) $430t_0$, hemifusion diaphragm; (f) $495t_0$, fusion pore appears; (g) $565t_0$, full fusion. Upper part: Section view. Different colors distinguish between lipid tail beads in the outer (blue and magenta) and the inner (green and yellow) monolayers for the two vesicles. Additionally, head beads of lipids in outer and inner monolayers are painted black and red respectively. Lower part: Perspective view. For better visibility, water and tail particles are omitted and head particles are shown in smaller size [42].

stalk expands radially and evolves into a hemifusion diaphragm (HD), in which two distal monolayers connect. Third, HD is degraded and a fusion pore appears. At last, the enlargement of water pore completes full fusion. Simultaneously the transmembrane segments (TMSs) of fusion protein complex in separate vesicles are coalesced into the same bilayer, and forms into cis-protein complex in the fused vesicle. These findings indicate that the fusion proteins serve as scaffolds to draw two membranes into close contact. Therefore this pathway is termed Scaffold model (pathway I). It is notable that the hemifusion intermediate and the fusion pore in this pathway are purely lipidic. Recent studies suggest that the TMSs of fusion proteins might contribute to the stalk-pore transition [32]. Our simulations show that if self-defined interactions are also imposed on TMSs, their association gives rise to an unstable protein-lined pore in hemifusion intermediate. As shown in Figure7(c), this fusion pore is partly composed of TMSs. Lipids and water can be incorporated into the pore, which allows the pore to expand instantly to accomplish membrane fusion. We name this pathway Protein-pore model (pathway II). For comparison, some parallel simulations with pure vesicles are performed. Several successful fusion events suggest that without the participation of proteins, the averaged fusion time is $150t_0$ close to that for pathway I, $140t_0$. Obviously pathway I and pure vesicle fusion undergo almost same fusion intermediates. The averaged fusion time for pathway II is $\sim 25t_0$, shorter than that through the pure lipidic pore intermediate. It indicates the formation of protein-lined pore promotes the stalk-pore transition and accelerates the fusion process. It is noted that due to a series of simplifications in our simulations, the fusion times cannot be transferred into real physical time directly. Additionally, there is no directly experiment evidence to support Pathway II. However we expect Pathway II is a new mechanism for protein-mediated membrane fusion, which needs further experimental confirmation.

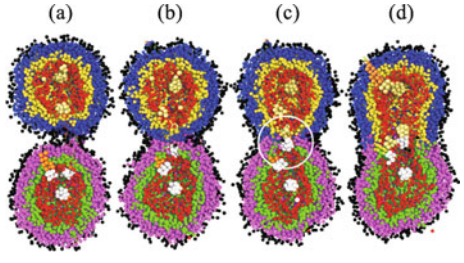

Figure 7 Pathway II of protein-mediated vesicle fusion (Protein-pore model). Protein-lined pore (encircled) originates directly from the radially expanding stalk, which allows lipid and water penetrate into it. Then the pore expands to accomplish vesicle fusion. (a) $225t_0$, outer leaflets contact; (b) $245t_0$, stalk; (c) 250 t_0, protein-lined fusion pore appears; (d) $275t_0$, full fusion. For clarity, water beads are omitted [42].

4 2D phase transformation in lipid bilayer

It's well known that lipid bilayers are the structural basis of all biologic membranes. Understanding the physics of lipid bilayers can yield insight into their biologic function, help to understand the cause of diseases, and eventually lead to the development of new therapeutics [69]. It have been proved that the lipid bilayer is the most useful model system to study the interactions of lipid membranes with other molecules, e.g., lipid-polymer interactions [70], lipid-protein interactions [71,72], lipid-DNA interactions [73,74]. Since the lipid molecules are restricted in membrane plane, the lipid bilayer is also a significantly perfect model of two-dimensional phase transition. As we known, the phase transition in two-dimension is quit different from that in three-dimension, which makes it rather attractive to researchers. It is found that lipid bilayers possess rich phase structures [75,76]. Although most biomembranes in living organisms are maintained in the fluid phase, both the pre-transition temperature and the main-transition temperature of some common bilayer lipids (such as DPPC) are close to the body temperature (35°C and 41°C), which make these phase transition has presumably some relevance for vital phenomena. Therefore the study of the phase transition in lipid bilayers is not only essential on theoretical research, but also on life science.

Lipid bilayers show various phase structures, even as the simplest model system is composed by only one kind of molecule [75,76]. As presented in Figure 8, the stable phase at low temperature is the sub-gel phase (L_C). With the increasing of temperature, it turns to the gel phases L_β or $L_{\beta'}$, which are differed by the tilt of the tail chains. The transition from the sub-gel phase to the gel phase is generally called as sub-transition. If head groups are large and weakly interacted, such as ether-linked phosphatidyl- cholines, the system adopts a $L_{\beta I}$ phase (Figure 8(c)), where both opposing lipid layers are fully interdigitated [75, 77–80]. On the one hand, both $L_{\beta'}$ and L_C phases are characterized by having a very low lipid mobility in the bilayer plane accompanied with the ordered tail chains, which can also be tilted with respect to the lipid bilayer normal. On the other hand, the head groups in the $L_{\beta'}$ phase are more hydrated than in the L_C phase, leading to some degree of disorder of tail chains in the $L_{\beta'}$ phase but a pronounced long range hexagonal lattice arrangement in the

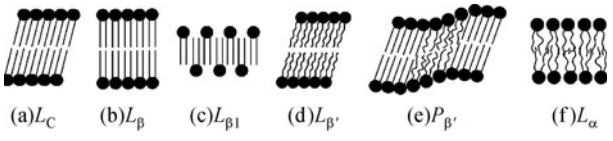

Figure 8 Schematical representations of the phase structures of the lipid bilayer [85].

bilayer plane in the L_C phase. Increasing temperature further results in the formation of the rippled ($P_{\beta'}$) phase which is characterized by a one-dimensional periodic height modulation of the bilayers [81–84]. The transition is denoted as the pre-transition. Finally, the bilayer undergoes a transition to the liquid crystalline or fluid L_α phase, which is called the main transition or the chain order/disorder transition. In this phase, the bilayer is a two-dimensional fluid, meaning that the lipids are free to move in the plane of the bilayer. The hydrocarbon chains become disordered and therefore the transition to the L_α phase is regarded as the melting of bilayers. A schematic illustration of these phase transition process is shown in Figure 9.

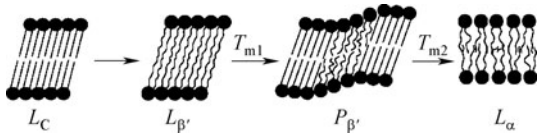

Figure 9 Schematical representations of the lipid bilayer phases during a heating process [86].

From an experimental point of view, studying the phase transformations of biomembranes on a molecular scale in situ is not an easy task [87,88]. As the dissipative particle dynamics simulation has been proved an efficient approach for bilayer simulation, Smit's group carried out a series of pioneering work on the phase behaviors of lipid bilayers with various architectures and compositions [43–48,68,85]. By varying the tail length, he first studied the influence of the tail length on the phase diagram. Three main phase regions appear on the phase diagrams: L_α, $L_{\beta I}$ and L_β. As the tail length increases, it is found that the gel phases are stabilized and the transitions of $L_\beta \rightarrow L_\alpha$ and $L_{\beta I} \rightarrow L_\alpha$ are shifted to higher temperatures. More significantly, they found that at a higher head-head repulsion the head group became more hydrated, the resulted larger projected area per head group makes the interdigitated phase $L_{\beta I}$ more stable. Later they tested on the double-tail lipid system, and built the phase diagrams for double-tail lipids with different tail lengths. As presented in Figure 10, at low values of the head-head repulsion parameter a_{hh}, with increasing temperature the bilayer undergoes the transitions from the subgel phase L_C via the flat gel phase L_β to the fluid phase L_α. While at higher values of a_{hh}, the transformation from the L_C to the L_α phase occurs through the tilted gel phase $L_{\beta'}$ and the rippled phase $P_{\beta'}$. Furthermore the $L_{\beta'}$ phase only exists for the long tail lipids. Although the nature of the rippled phase is not yet clear, it can be seen from

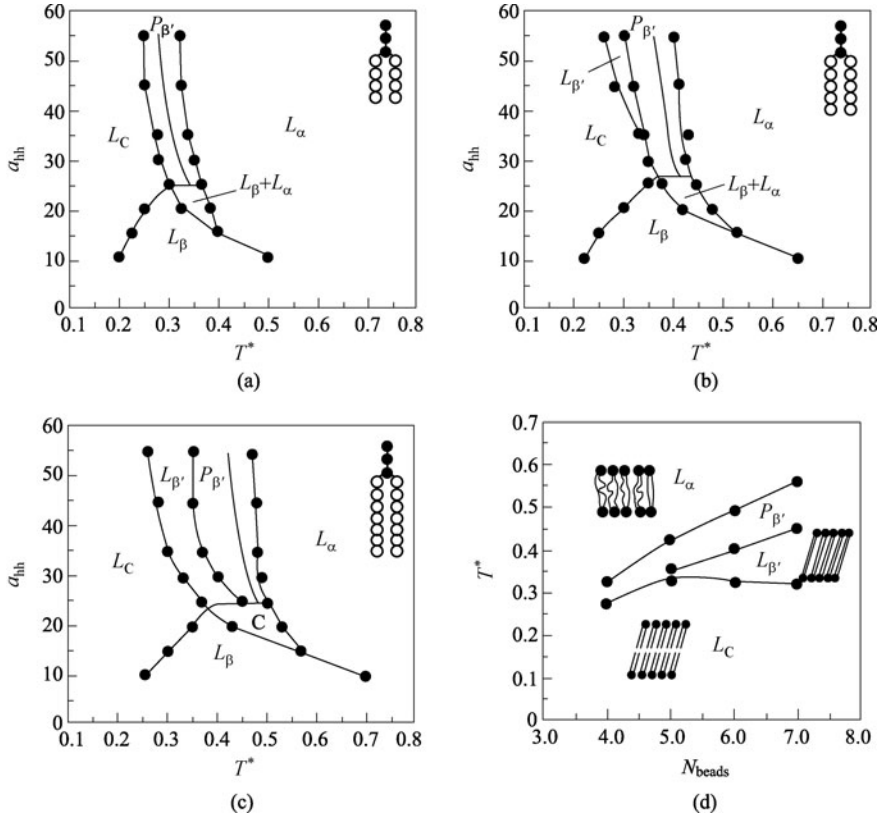

Figure 10 Phase behavior as a function of the temperature and head group interactions for (a) $h_3(t_4)_2$, (b) $h_3(t_5)_2$, and (c) $h_3(t_6)_2$. The transition temperatures as a function of tail length for the typical head-head interactions (a_{hh} = 35) are shown in (d) [85].

Figure 10 that the rippled structure ($P_{\beta'}$) is expected when the head groups are sufficiently surrounded by water. In agreement with experimental observations that rippled phase is a coexistence phase between L_C or $L_{\beta'}$ and L_α, it exhibits an asymmetric sawtooth with a difference in thickness between the long and the short arm [84]. Similar to the single-tail lipids, at high a_{hh} the head groups prefer to be hydrated strongly, the resulted larger area per lipid drives those tilted tails phases (L_C or $L_{\beta'}$) more stable. In contrast, at low a_{hh}, the head-head contacts become favorable, water is expelled from the head group region, the resulted smaller area per lipid drive the tails more ordered and straighter, consequently the L_β phase is evolved. It is worthy to note that the phase diagrams in Figure 10 do not include any interdigitated phases, although they were found in several systems experimentally [75,77–80]. Inspired by the results from the single-tail lipids that the interdigitated phase could be stabilize by increasing distance between neighboring head groups, Smit's group built an ingenious approach to locate them. They added small molecule alcohol into the double-tail lipid systems and recovered the experimentally observed interdigitated phase $L_{\beta I}$ at high alcohol concentrations [46].

Despite the large number of thermodynamic as well as composition parameters, among the major issue concerning the phase behavior of lipid bilayers are the architecture of lipid molecule. Given this, we investigated the phase behavior of the double-tail lipid bilayers we previously employed [89]. As presented in Figure 11, the main difference lies in the linkage of the head groups to tails comparing with Smit's model. Although the primary motivation of the previous two sections is the study of fluid phases, by building the phase diagram we can map out regions of fluid behavior within the studied parameter space. The derived phase diagram is exhibited in Figure 12. Distinctions between Figure 12 and the corresponding phase diagram of Figure 10(b) done by Smit are rather significant. First, we obtain an interdigitated structure. As expected from Figure 11, our lipid model has an obviously larger area of head-group than Smit's model, the appearance of interdigitated structure in our system is surely reasonable because the interdigitated phase is well stabilized by larger

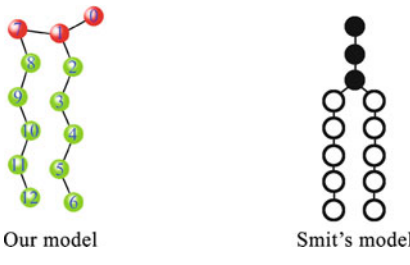

Figure 11 Models of the lipids used in our simulation and Smit's.

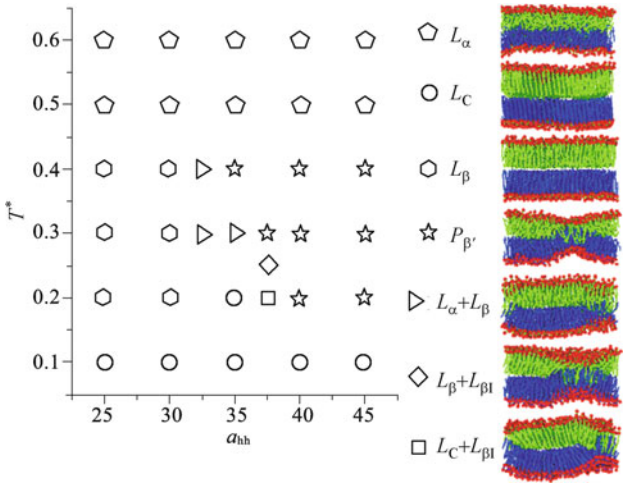

Figure 12 Phase diagram of $h_3(t_5)_2$ as a function of reduced temperature T^* and head-head repulsion parameter a_{hh}.

area of head-group. Second, in contrast to Smit, we have not obtained a tilt gel phase $L_{\beta'}$. Smit attributed the occurrence of $L_{\beta'}$ phase to the long tail effect. Therefore, as shown in Figure 10, $L_{\beta'}$ diminishes at the tail length less than 5, and only appears in a very narrow region at the tail length of 5. In our model the low aspect ratio resulting from the larger head area will further reduce the chance of $L_{\beta'}$ phase even at the same tail length of 5. Third, the phase transition to L_C occurs at a lower temperature. Fourth, we observe a very wide region of the $P_{\beta'}$ ripple phase, almost twice the size of the $P_{\beta'}$ region shown in Figure 10(b). The larger head projection area in our model is susceptible to the strong head-water contact. The phenomenon of preference to the ripple phase confirms the fact that the ripple phase is related with the head-water contact. Detailed calculations show that each phase possesses the distinguished structural properties such as chain conformation and membrane size, which helps us to locate the phase boundary. By applying the quasi-heating or quasi-cooling process, we explore the kinetic path of both $L_C \rightarrow L_\beta \rightarrow L_\alpha$ transition at weak head-head repulsion and $L_C \rightarrow P_{\beta'} \rightarrow L_\alpha$ transitions at strong head-head repulsion.

Since the ripple phase is intermediate between the fluid and gel phases, study of its properties will improve the understanding of coupling between the lipid matrix and the resulted molecular organization. These insights are likely to be relevant to the order-disorder transition in a broad sense. But there is still a question about how to distinguish the ripple phase from coexistence phase. For example, we cannot differ the ripple phase (presented in Figure 13(b)) from the ordinarily coexistence phase (presented in Figure 13(a)) by configuration observations. Because both the normal coexistence phase and the ripple phase show an inconsistency of

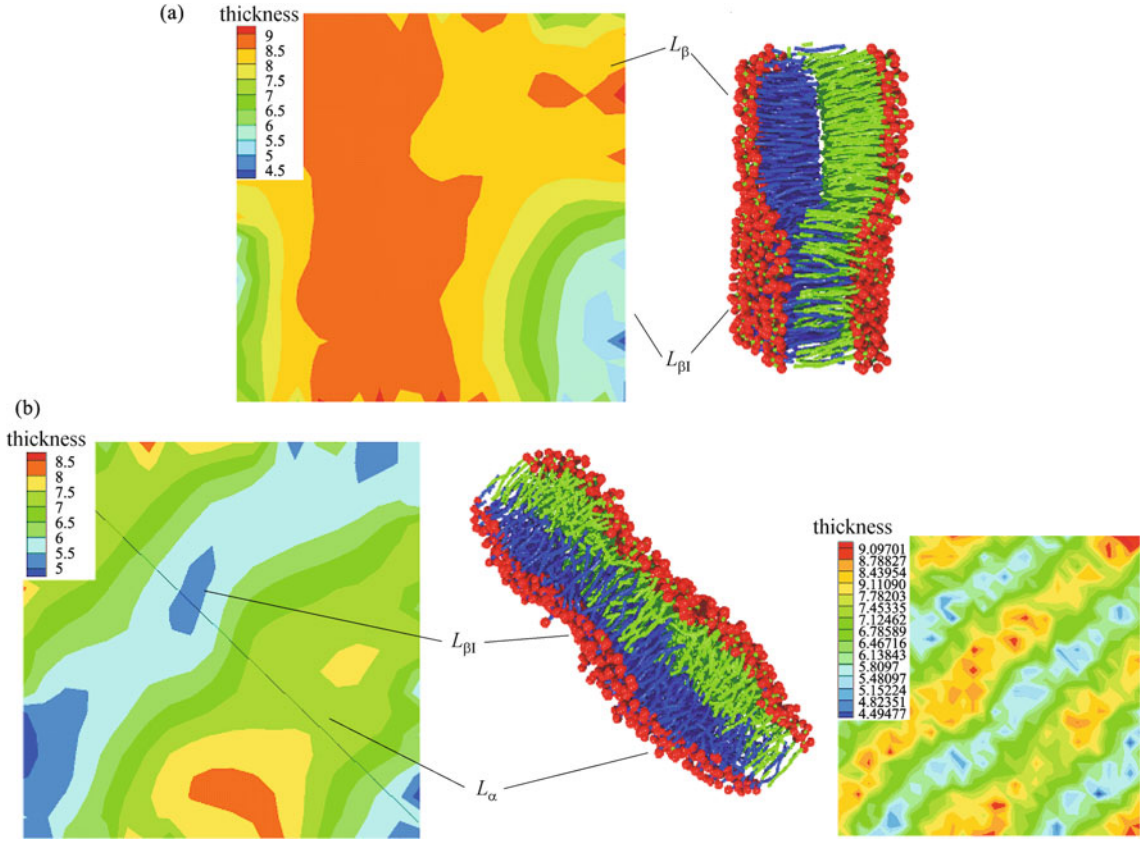

Figure 13 (a) $L_\beta + L_{\beta I}$ at $T^* = 0.2$ and $a_{hh} = 40$; Left: thickness of the membrane as a function of the position in the plane where the color coding gives the thickness of the bilayer membrane. Right: side view in which the head groups are red and the tails blue or green dependent on different layer. (b) $P_{\beta'}$ at $T^* = 0.4$ and $a_{hh} = 40$; Left: thickness profile. Middle: side view of lipid bilayer. Right: thickness profile for the 4-fold system size of the left one).

structure and thermodynamic properties, it is not easy to accurately define them from structure data and thermodynamic observables. Therefore, to characterize the ripple phase and to signify its nature of a one-dimensional periodic height modulation of the bilayers, we measure the height distribution profiles for bilayers.

5 Conclusion

Both the lipid bilayer and its enclosed partner-vesicle are the satisfactory models for the cellular membrane from a biologic point of view. In this paper we have reviewed the current simulation progress on vesicle dynamics including vesicle formation and (protein-mediated) vesicle fusion, as well as the phase transition in lipid bilayers. We find that the minimization of hydrophobic energy is the main driving force for the bilayer-vesicle transition. Then we make the first attempt using a simple model system to mimic the complicated protein-mediated vesiclefusion involving extensive and cooperative molecular rearrangement. Fusion proteins are introduced as the fusion machines. The "zippering" of protein complexes brings separate vesicles into close proximity and catalyzes their fusion. The subsequent fusion pathway generally follows the stalk-pore mechanism, in which the stalk intermediate and the fusion pore are purely lipidic. However, if the protein pairs "zipper" through their TMSs, the fusion pore originates directly from the radially expanding stalk, which promotes the stalk-pore transition and speeds up fusion further. At last the phase diagram of lipid bilayers is built. Among the large number of thermodynamic and composition parameters, the phase structures are most sensitive to the architecture of lipid molecule. By comparing the two different double-tail lipid models, it is found that the experimentally observed interdigitated phase and ripple phase are well stabilized by larger area of head-group.

Acknowledgements The work was supported by the National Natural Science Foundation of China (Grant No. 20674093).

References

1. Gennis, R. B., *Biomembranes*, Springer-Verlag: New York, 1989
2. Ortiz, V.; Nielsen, S. O.; Discher, D. E.; Klein, M. L.; Lipowsky,

R.; Shillcock, J., *J. Phys. Chem. B* **2005**, *109*, 17708–17714
3. Wang, H.; Nieh, M. P.; Hobbie, E. K.; Glinka, C. J.; Katsaras, J., *Phys. Rev. E* **2003**, *67*, 060902
4. Marrink, S. J.; Lindahl, E.; Edholm, O.; Mark, A. E., *J. Am. Chem. Soc*. **2001**, *123*, 8638–8639
5. Imparato, A.; Shillcock, J. C.; Lipowsky, R. *Eur. Phys. J. E* **2003**, *11*, 21–28
6. Lipowsky, R., *Curr. Opin. Struct. Biol*. **1995**, *5*, 531–540
7. Tanford, C., *Proc. Natl. Acad. Sci. USA* **1979**, *76*, 4175–4176
8. Tanford, C., *Science* **1978**, *200*, 1012–1018
9. Venturoli, M.; Sperotto, M. M.; Kranenburg, M.; Smit, B., *Phys. Rep*. **2006**, *437*, 1–54
10. Simões, S.; Moreira, J. N.; Fonseca, C.; Düzgüneş, N.; de Lima, M. C., *Adv. Drug Deliv. Rev*. **2004**, *56*, 947–965
11. Lipowsky, R.; Gillessen, T.; Alzheimer, C., *J. Neurophysiol*. **1996**, *76*, 2181–2191
12. Hitz, T.; Luisi, P. L., *Biopolymers* **2000**, *55*, 381–390
13. Yamamoto, S.; Maruyama, Y.; Hyodo, S., *J. Chem. Phys*. **2002**, *116*, 5842–5849
14. Lipowsky, R.; Baumgärtner, A., *Phys. Rev. A* **1989**, *40*, 2078–2081
15. de Vries, A. H.; Mark, A. E.; Marrink, S. J., *J. Am. Chem. Soc*. **2004**, *126*, 4488–4489
16. Leng, J.; Egelhaaf, S. U.; Cates, M. E., *Europhys. Lett*. **2002**, *59*, 311–317
17. Bernardes, A. T., *Langmuir* **1996**, *12*, 5763–5767
18. Marrink, S. J.; Mark, A. E., *J. Am. Chem. Soc*. **2003**, *125*, 15233–15242
19. Markvoort, A. J.; Pieterse, K.; Steijaert, M. N.; Spijker, P.; Hilbers, P. A. J., *J. Phys. Chem. B* **2005**, *109*, 22649–22654
20. Noguchi, H.; Takasu, M., *Phys. Rev. E* **2001**, *64*, 041913
21. Shillcock, J. C.; Lipowsky, R., *Nat. Mater*. **2005**, *4*, 225–228
22. Shelley, J. C.; Shelley, M. Y.; Reeder, R. C.; Bandyopadhyay, S.; Klein, M. L., *J. Phys. Chem. B* **2001**, *105*, 4464–4470
23. Yamamoto, S.; Hyodo, S., *J. Chem. Phys*. **2003**, *118*, 7937–7943
24. Bernardes, A. T., *J. Phys. II France* **1996**, *6*, 169–174
25. Marrink, S. J.; Mark, A. E., *J. Am. Chem. Soc*. **2003**, *125*, 11144–11145
26. Knecht, V.; Marrink, S. J., *Biophys. J*. **2007**, *92*, 4254–4261
27. Cohen, F. S.; Melikyan, G. B., *J. Membr. Biol*. **2004**, *199*, 1–14
28. Yang, L.; Huang, H. W., *Science* **2002**, *297*, 1877–1879
29. Jackson, M. B.; Chapman, E. R., *Annu. Rev. Biophys. Biomol. Struct*. **2006**, *35*, 135–160
30. Jahn, R.; Grubmüller, H., *Curr. Opin. Cell Biol*. **2002**, *14*, 488–495
31. Li, D. W.; Liu, X. Y., *J. Chem. Phys*. **2005**, *122*, 174909
32. Han, X.; Wang, C. T.; Bai, J.; Chapman, E. R.; Jackson, M. B., *Science* **2004**, *304*, 289–292
33. Lindahl, E.; Edholm, O., *Biophys. J.* **2000**, 79, 426–433
34. Nielsen, S. O.; Lopez, C. F.; Srinivas, G.; Klein, M. L., *J. Phys.*: *Condens. Matter* **2004**, *16*, R481–R512
35. Lipowsky, R.; Sackmann, E., *Structure and Dynamics of Membranes, Handbook of Biological Physics, Vol. 1*, Elsevier: Amsterdam, 1995
36. Lipowsky, R., *Nature* **1991**, *349*, 475–481
37. Jülicher, F.; Lipowsky, R., *Phys. Rev. Lett*. **1993**, *70*, 2964–2967
38. Umeda, T.; Nakajima, H.; Hotani, H., *J. Phys. Soc. Jpn*. **1998**, *67*, 682–688
39. Wu, S. G.; Guo, H. X., Beijing: Institute of Chemistry, Chinese Academy of Sciences, Doctoral thesis, 2009
40. Li, X. J.; Liu, Y.; Wang, L.; Deng, M. G.; Liang, H. J., *Phys. Chem. Chem. Phys*. **2009**, *11*, 4051–4059
41. Li, X. J.; Pivkin, I. V.; Liang, H. J.; Karniadakis, G. E., *Macromolecules* **2009**, *42*, 3195–3200
42. Wu, S. G.; Guo, H. X., *J. Phys. Chem. B* **2009**, *113*, 589–591
43. Venturoli, M.; Smit, B., *PhysChemComm* **1999**, *2*, 45–49
44. Kranenburg, M.; Venturoli, M.; Smit, B., *Phys. Rev. E* **2003**, *67*, 060901
45. Kranenburg, M.; Laforge, C.; Smit, B., *Phys. Chem. Chem. Phys*. **2004**, *6*, 4531–4534
46. Kranenburg, M.; Smit, B., *FEBS Lett*. **2004**, *568*, 15–18
47. Kranenburg, M.; Vlaar, M.; Smit, B., *Biophys. J*. **2004**, *87*, 1596–1605
48. Kranenburg, M.; Venturoli, M.; Smit, B., *J. Phys. Chem. B* **2003**, *107*, 11491–11501
49. Venturoli, M.; Sperotto, M. M.; Kranenburg, M.; Smit, B., *Phys. Rep*. **2006**, *437*, 1–54
50. Klein, M. L.; Raviv, U.; Perkin, S.; Kampf, N.; Chai, L.; Giasson, S., *J. Phys.*: *Condens. Matter* **2004**, *16*, R481–R512
51. Müller, M.; Katsov, K.; Schick, M., *Phys. Rep*. **2006**, *434*, 113–176
52. Safran, S. A.; Pincus, P. A.; Andelman, D.; MacKintosh, F. C., *Phys. Rev. A* **1991**, *43*, 1071–1078
53. Kumaran, V. J., *Chem. Phys*. **1993**, *99*, 5490–5499
54. Morse, D. C.; Milner, S. T., *Europhys. Lett*. **1994**, *26*, 565–570
55. U. Seifert, *Fluid Membranes-Theory of Vesicle Conformations*; Habilitation Theses, Jü lich: Institut Für Festkörperforschung, 1994
56. Porte, G.; Ligoure, C. J., *J. Chem. Phys*. **1995**, *102*, 4290–4298
57. Fattal, D. R.; Andelman, D.; Ben-Shaul, A., *Langmuir* **1995**, *11*, 1154–1161
58. Wu, S. G.; Guo, H. X., *Sci. China B* **2008**, *51*, 743–750
59. Rawicz, W.; Olbrich, K. C.; McIntosh, T.; Needham, D.; Evans, E., *Biophys. J*. **2000**, *79*, 328–339
60. Jahn, R.; Lang, T.; Südhof, T. C., *Cell* **2003**, *112*, 519–533
61. Noguchi, H.; Takasu, M. J., *J. Chem. Phys*. **2001**, *115*, 9547–9551
62. Müller, M.; Katsov, K.; Schick, M. J., *J. Chem. Phys*. **2002**, *116*, 2342–2345
63. Stevens, M. J.; Hoh, J. H.; Woolf, T. B., *Phys. Rev. Lett*. **2003**, *91*, 188102
64. Kozlovsky, Y.; Chernomordik, L. V.; Kozlov, M. M., *Biophys. J*. **2002**, *83*, 2634–2651
65. Kuzmin, P. I.; Zimmerberg, J.; Chizmadzhev, Y. A.; Cohen, F. S., *Proc. Natl. Acad. Sci. USA* **2001**, *98*, 7235–7240
66. Smeijers, A. F.; Markvoort, A. J.; Pieterse, K.; Hilbers, P. A. J., *J. Phys. Chem. B* **2006**, *110*, 13212–13219
67. Hughson, F. M., *Curr. Biol*. **1999**, *9*, R49–R52

68. Venturoli, M.; Smit, B.; Sperotto, M. M., *Biophys. J*. **2005**, *88*, 1778–1798
69. Sperotto, M. M.; May, S.; Baumgaertner, A., *Chem. Phys. Lipids* **2006**, *141*, 2–29
70. Freyssingeas, E.; Antelmi, D.; Kekicheff, P.; Richetti, P.; Bellocq, A. M., *Eur. Phys. J. B* **1999**, *9*, 123–136
71. Koltover, I.; Rädler, J. O.; Salditt, T.; Rothschild, K. J.; Safinya, C. R., *Phys. Rev. Lett*. **1999**, *82*, 3184–3187
72. Münster, C.; Lu, J.; Schinzel, S.; Bechinger, B.; Salditt, T., *Eur. Biophys. J*. **2000**, *28*, 683–688
73. Rädler, J. O.; Koltover, I.; Salditt, T.; Safinya, C. R., *Science* **1997**, *275*, 810–814
74. Artzner, F.; Zantl, R.; Rapp, G.; Rädler, J. O., *Phys. Rev. Lett*. **1998**, *81*, 5015–5018
75. Koynova, R.; Caffrey, M., *Biochim. Biophys. Acta* **1998**, *1376*, 91–145
76. Stümpel, J.; Eibl, H.; Nicksch, A., *Biochim. Biophys. Acta* **1983**, *727*, 246–254
77. Lohner, K.; Schuster, A.; Degovics, G.; Müller, K.; Laggner, P., *Chem. Phys. Lipids* **1987**, *44*, 61–70
78. Koynova, R.; Caffrey, M., *Chem. Phys. Lipids* **1994**, *69*, 1–34
79. Ichimori, H.; Hata, T.; Matsuki, H.; Kaneshina, S., *Biochim. Biophys. Acta* **1998**, *1414*, 165–174
80. Kusube, M.; Tamai, N.; Matsuki, H.; Kaneshina, S., *Biophys. Chem*. **2005**, *117*, 199–206
81. MacKintosh, F. C., *Curr. Opin. Colloid Interface Sci*. **1997**, *2*, 382–387
82. Janiak, M. J.; Small, D. M.; Shipley, G. G., *Biochemistry* **1976**, *15*, 4575–4580
83. Czajkowsky, D. M.; Huang, C.; Shao, Z., *Biochemistry* **1995**, *34*, 12501–12505
84. Leidy, C.; Kaasgaard, T.; Crowe, J. H.; Mouritsen, O. G.; Jørgensen, K., *Biophys. J.* **2002**, *83*, 2625–2633
85. Kranenburg, M.; Smit, B., *J. Phys. Chem. B* **2005**, *109*, 6553–6563
86. Kranenburg, M., *Phase Transitions of Lipid Bilayers: Amesoscopic Approach*, University of Amsterdam: Netherlands, 2004
87. Münster, C.; Salditt, T.; Vogel, M.; Siebrecht, R.; Peisl, J., *Europhys. Lett*. **1999**, *46*, 486–492
88. Salditt, T.; Münster, C.; Mennicke, U.; Ollinger, C.; Fragneto, G., *Langmuir* **2003**, *19*, 7703–7711
89. Lu, T.; Wu, S. G.; Guo, H. X., *J. Phys. Chem. B* (submitted)